MOLECUALR DOCKING, HARSHIEFIELD SURFACE AND REACTIVITY AND HYPERPOLARIZABILITY ANALYSIS OF 3-(2-BROMOACETYL)-2H-CHROMEN-2-ONE

Loice Bessylet [1,2] , Gnana Sampantham [3] , M.Amalanathan [4] , Usha [5] and M. Sony Michael Mary [6]
[1] Research Scholar, Reg.No:12114, Manonmaniam Sundaranar University, Abishekapatti Tirunelveli-627012, Tamil Nadu, India
[2] Department of Physics, Udaya College of Arts and Science, Ammandivilai (PO), Kanyakumari - 629 204, Tamil Nadu, India
[3] Department of Physics, S.T Hindu College – Nagercoil - 629002, Tamil Nadu, India
[4] Department of Physics, Nanjil Catholic College of Arts and Science, Kaliyakkavilai- 629153, Tamil Nadu, India
[5] Department of Physics, Women's Christian College, Nagercoil – 629001, Tamil Nadu, India
[6]Department of Physics & Research Centre, Nesamony Memorial Christian College, Marthandam, 629165 TamilNadu, India

ABSTRACT:

The molecular geometrical, molecular static polarizability and hyperpolarizability parameters, Molecular Hirshfeld molecular docking analysis as well as HOMO-LUMO energies of 3-(2-bromoacetyl)-2H-chromen-2-one in the ground state were examined using DFT levels of density functional theory) with 6-311++G(d,p) basis set. The enormous enhancement of the hyperpolarizability reveals that these classes of organic compounds show very large non-linear optical properties and hence in general may influence in finding and developing the potential non-linear optical materials. The frontier molecular orbital calculation clearly shows the inverse relationship of HOMO–LUMO gap with the total static hyperpolarizability. Antibacterial and antifungal activity of the molecule also identified in order to prove the bioactivity of the molecule. The Possible interaction with in the molecule is identified by Molecular Hirshfeld analysis.

Index term: Polarizability and Hyperpolarizability, Harshifield, Molecular Docking, HOMO-LUMO.

I. INTRODUCTION

Coumarin is a chemical compound which is found naturally in some plants. Coumarin is found in a variety of plants such as tonka bean, vanilla grass, woodruff, mullein, sweet grass, lavender, sweet clover grass, and licorice, and also occurs in food plants such as strawberries, apricots, cherries, and cinnamon. It can be synthetically produced as well. It has a distinctive odor, which has led people to use it as a food additive and ingredient in perfume. Due to concerns about coumarin as a potential liver and kidney toxin, its use as a food additive is heavily restricted, although it is perfectly safe to eat foods which naturally contain coumarin [1,2]. Coumarins are an important class of compounds because of their applications in synthetic chemistry, medicinal chemistry and photochemistry. Some coumarins are photoactive; they are also widely used in organic solid chemistry [3,4], laser dyes [5,6], biological sensors [7] and molecular switches [8]. Coumarins exhibit antiviral [9] and antimicrobial activities [10]. Coumarins generate strong interest stemming from their great physiological and biological activities, which is further exemplified by their roles as anticoagulants (dicoumarols and its derivatives, warfarin), spasmolytics [11], chemotherapeutics [12], biological inhibitors.

Nonlinear optic is at the forefront of current research because of its importance in providing the key functions of optical modulation, optical logic, optical switching, optical memory and frequency shifting for the emerging technologies in areas such as optical interconnections, signal processing and telecommunications [13]. The crystal engineering strategy of combining organic and inorganic moieties was proposed to produce materials having noncentrosymmetric structures, good stabilities and high nonlinear coefficients. Several examples of hybrid organic inorganic crystals have emerged as good candidates for NLO materials [14-17]. Molecular dipole moments, polarizabilities and hyperpolarizabilities are widely studied, both experimentally and theoretically,m due to their importance in designing new electrical and optical materials. Experimentally hyperpolarizabilities can be measured in both gas and liquid phases by dc electric field induced second harmonic generation. Density functional theory calculations of polarizabilities and hyperpolarizabilities for small molecules have proven to be in good to reasonable agreement with results obtained from wave function based correlated methods and gas phase experiments [18–21].The structural and Vibratinal analysis of 3-(Bromoacetyl)Coumarin was already reported[22]. In my best of knowledge the First and second order hypaerpolariability of 3-(2-bromoacetyl)-2H-chromen-2-one(BAC) was not yet reported. The present work describes the effect of charge transfer interaction in vibrational spectrum, first and second Order Hyperpolarizability, Harshiefield investigations of BAC aided by density functional computations to elucidate the correlation between the molecular structure and activity. Molecular docking was performed with various proteins and docking parameters were obtained

II. COMPUTATIONAL DETAILS

The ab initio quantum mechanical calculations were carried out using the Gaussian 09W programs [23]. Initial geometry generated from standard geometrical parameter was minimized without any constraint in the potential energy surface at HF, adopting the standard 6-31G (d,p) basis set. This geometry was then re optimized at three parameter hybrid functional (B3) Lee–Young–Parr(LYP) level using 6-311++G(d,p) basis set[24-27]. The Dipole moment, static polarizability, dynamic polarizability , First and second order hyperpolarizabilities were calculated at the DFT level. AutoDock Suite 4.2.1 was used to find the minimum binding energy, inhibition constant and various parameters of the ligand-protein docking interactions. The identification of biological activity is conformed to antibacterial and antifungal activity. The molecular geometry of the present compound is calculated at B3LYP level with 6-311++G (d,p). The optimized structure shows minimum energy conformation compare to the other levels of computation. The atom numbering scheme adopted in this study is given in Figure 1.

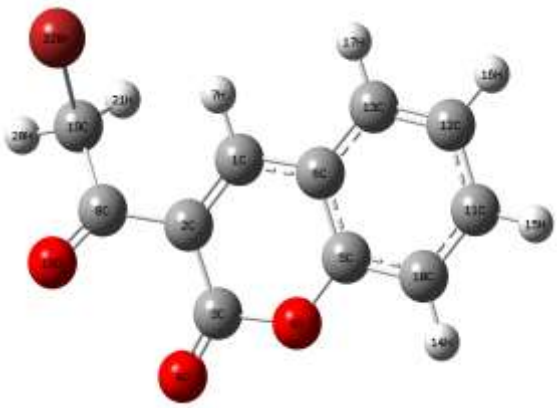

Figure 1: Optimized Structure of 3BAC

III. NON LINEAR OPTICAL ANALYSIS

Density functional theory has been used as an effective method to investigate the organic non-linear optical (NLO) materials. Recent research works have illustrated that the organic non-linear optical materials are having high optical non-linearity than inorganic materials [21]. In the presence of an applied electric field, the energy of a system is a function of the electric field. Polarizabilities and

hyperpolarizabilities characterize the response of a system in an applied electric field [22]. It determine not only the strength of molecular interactions but also the cross sections of different scattering and collision processes, as well as the NLO properties of the system [23-25]. The dipole moment, polarizabilities and hyperpolarizabilities characterize the response of a system in an applied electric field[26,27]. Electric polarizability is a fundamental characteristic of atomic and molecular systems[28]. Dipolemoment polarizabilities and hyperpolarizabilities could determine not only the strength of molecular interactions (such as the ong-range intermolecular induction, and dispersion forces), the cross sections of different scattering and collision processes, but also the NLO of the system[29]. The theory of electric polarizability is a key element of the rational interpretation of a wide range of phenomena, from nonlinear optics[30 and electron scattering [31]to phenomena induced by intermolecular interactions[32-35]. In the present investigations, the electronic dipole moment, molecular polarizability, anisotropy of polarizability, molecular first hyperpolarizability and second hyperpolarizabilities of present compound were investigated. The electric dipole moment μ, polarizability α, the hyper polarizability β and first order hyperpolarizability γ of the of title compound are calculated by finite field method using B3LYP/6-311++G(d,p) basis set available in Gaussian 09 package.

Table 1a: Calculated Dipole moment component and the totoal dipole moment of 3BAC

Dipole Moment Component	3-(Bromoacetyl)Coumarin				Urea
	HF/6-31G(d)	B3LYP/6-31G(D)	B3LYP/CC-PVZ	B3LYP6-311++G(d,p)	
μ_{xx}	0.169	0.285	0.257	0.257	1.282
μ_{yy}	-0.742	-0.621	-0.588	-0.636	0.00004
M_{zz}	-2.964	-2.541	-2.418	-2.728	-0.83
	2.06 Debye	**2.63 Debye**	**2.50 Debye**	**2.81 Debye**	**1.52 Debye**

The dipole moment, polarizabilities first hyperpolarizability (βo) and related properties (μ, αo, Δα βand γ) are calculated based on the finite- field approach. In the presence of an applied electric field, the energy of a system is the function of the electric field. The first hyperpolarizability is a third - rank tensor that can be described by a 3 x 3 x 3 matrix. The 27 components of the 3D matrix can be reduced to 10 components due to the Kleinman symmetry[36]. The components of β are defined as the coefficients in the Taylor series expansion of the energy in the external electric field. When the electric field is weak and homogeneous, this expansion becomes.

$$E = E^{\circ} - \mu_i F_i - \tfrac{1}{2} \alpha_{ij} F_i F_j - \tfrac{1}{6} \beta_{ijk} F_i F_j F_k - \tfrac{1}{24} \gamma_{ijkl} F_i F_j F_k F_l + \ldots\ldots \quad (1)$$

where E^{o} is the energy of the unperturbed molecules, F_i is the field at the origin μ_i □□ α_{ij} , β_{ijk} and γ_{ijkl} are the components of dipole moment, polarizabiltiy, first and second order hyperpolarizability respectively. These studies led to the fact that ab initio calculations of polarizabilities and hyperpolarizabilities have become available through the strong theoretical basis for analyzing molecular interactions. They made possible the determination of the elements of these tensors from derivatives of the dipole moment with respect to the electric field. The total static dipole moment μ, the mean polarizability α_0, the anisotropy of the polarizability Δα and the mean first hyperpolarizability βo, using the x-, y- and z- components are defined as

$$\mu = (\mu_x^2 + \mu_y^2 + \mu_z^2)^{1/2}$$

Dipole moment μ, of 3BAC calculated at the HF/631 G(d), B3LYP/6-31G(D), B3LYP/CC-PVZ and B3LYP/6-311G++(d,p) level of theory and Urea calculated at B3LYP/6-311G++(d,p) and are shown in Table 1. From the table it shows that the dipole moment calculated at B3LYP/6-311G++(d,p) is greater than the other level. The calculated dipole moment of 3BAC is also greater than urea.

The results for dipole moment, presented in Table 1a show that the basis set B3LYP6-311++G(d,p) and the B3LYP/CC-PVZ provides the largest and the smallest value for dipole moment respectively. The addition of d-polarization functions tends to increase in

the total magnitude of total dipole moment, while the p-polarization functions have negligible impact. From this one can say that diffuse and polarization functions lead to similar trends for a mean dipole moment calculation.

Table 1b: Calculated Dipole moment component and the Polarizability of 3BAC

Polarizability Components	3-(Bromoacetyl)Coumarin				Urea
	HF/6-31G(d)	B3LYP/6-31G(D)	B3LYP/CC-PVZ	B3LYP/ 6-11++G(d,p)	
α_{xx}	157.48	177.80	180.78	197.97	39.26
α_{xy}	-4.32	-4.21	-4.28	-4.50	0.294
α_{yy}	63.54	63.76	66.13	90.78	24.69
α_{xz}	-26.47	-34.49	-35.03	-35.39	-1.159
α_{yz}	-4.51	-4.39	-5.17	-3.94	0.45
α_{zz}	179.59	188.58	190.47	209.72	38.219
α_0	**1.97×10^{-23}**	**2.12×10^{-23}**	**$2.\times10^{-23}$**	**2.46×10^{-23}**	**5.04×10^{-23}**
$\Delta\alpha$	**2.09×10^{-23}**	**2.37×10^{-23}**	**2.37×10^{-23}**	**2.57×10^{-23}**	**2.52×10^{-23}**

The total static the mean polarizability α_0, the anisotropy of the polarizability $\Delta\alpha$ and the mean first hyperpolarizability βo, using the x-, y- and z- components are $\mu = (\mu_x^2 + \mu_y^2 + \mu_z^2)^{1/2}$

$$\alpha_0 = (\alpha_{xx} + \alpha_{yy} + \alpha_{zz})/3$$

$$\Delta\alpha = 2^{-1/2}[(\alpha_{xx} - \alpha_{yy})^2 + (\alpha_{yy} - \alpha_{zz})^2 + (\alpha_{zz} - \alpha_{xx})^2 + 6\alpha_{xz}^2]^{1/2} \quad (2)$$

The first order hyperpolarizability β was also calculated using the finite field approach theory [25]. The components of first hyperpolarizability can be calculated using the following equation

$$\beta_i = \beta_{iii} + \frac{1}{3}\sum\left(\beta_{ijj} + \beta_{jij} + \beta_{jji}\right), (i \neq j)$$

Using the x,y and z components, the magnitude of the first hyperpolarizability tensor can be calculated using

$$\beta_{tot} = (\beta_x^2 + \beta_y^2 + \beta_z^2)^{1/2} \quad (3)$$

The complete equation for calculating the magnitude of the first hyperpolarizability from Gaussian 09 output is as follows.

$$\beta = \left[\left(\beta_{xxx} + \beta_{xyy} + \beta_{xzz}\right)^2 + \left(\beta_{yyy} + \beta_{yzz} + \beta_{yxx}\right)^2 + \left(\beta_{zzz} + \beta_{zxx} + \beta_{zyy}\right)^2\right]^{\frac{1}{2}} \quad (4)$$

The second hyperpolarizability γ has been calculated only with semiempirical methods[26] . The equation for average second hyperpolarizability is

$$\langle\gamma\rangle = \frac{1}{5}\left(\gamma_{xxxx} + \gamma_{yyyy} + \gamma_{zzzz} + 2\gamma_{xxyy} + 2\gamma_{xxzz} + 2\gamma_{yyzz}\right) \quad (5)$$

Table 1c: Calculated Dipole moment component and the Hyper Polarizability of 3BAC

Hyper Polarizability Components	3-(Bromoacetyl)Coumarin				Urea
	HF/6-31G(d)	B3LYP/6-31G(D)	B3LYP/CC-PVZ	B3LYP/ 6-11++G(d,p)	
β_{xxx}	-392.47	-665.77	-609.742	-850.51	24.729
β_{xxy}	-2.74	3.38	-20.1795	24.49	-0.499
β_{xyy}	-3.66	-12.59	-11.9216	6.41	31.817
β_{yyy}	-20.66	-20.21	-43.9051	-3.34	0.0066
β_{xxz}	347.26	461.71	440.473	504.98	-61.443
β_{xyz}	-1.13	-5 .62	1.611872	-10.27	-0.225
β_{yyz}	-10.04	-9.57	-16.2812	-93.39	-20.593
β_{xzz}	-173.69	-244.57	-227.943	-290.74	19.374
β_{yzz}	-12.05	-5.03	-14.1506	-10.61	0.5057
β_{zzz}	-218.33	-99.68	-150.186	-130.78	32.896
	583.1765	**988.194**	**896.1202**	**1169.12268**	**90.43554**
β_{total}	**5 x10^{-30}**	**9 x10^{-30}**	**8 x10^{-30}**	**1.01 x10^{-29}**	**8 x10^{-31}**

The polarizability, hyperpolarizablity, second order hyperpolarizability components of 3BAC and urea calculated at different level is given the table b, c and d,. The variation on dipole moment, polariability and hyperpolarizabilities are compared with different level is shown in the figure 2 The results for static polrizability, dynamic polarizability and hyperpolarizabilities, presented in Table 1 show that the basis set B3LYP6-311++G(d,p) and the B3LYP/CC-PVZ provides the largest and the smallest value for respectively. The calculated DFT level static polrizability, dynamic polarizability and hyperpolarizabilities are larger than the HF value. Also the addition of d-polarization functions tends to increase in the total magnitude of total dipole moment, while the p-polarization functions have negligible impact. From this one can say that diffuse and polarization functions lead to similar trends for a mean dipole moment calculation.

Table 1d: Calculated Dipole moment component and the Second order Hyper Polarizability of 3BAC

Second order Hyper Polarizability Components	3-(Bromoacetyl)Coumarin				Urea
	HF/6-31G(d)	B3LYP/6-31G(D)	B3LYP/CC-PVZ	B3LYP/ 6-11++G(d,p)	
γ_{xxxx}	5.98	5.33	5.16	5.86	-0.23519
γ_{xxyy}	1.172	0.86	0.74	1.05	-1.8785
γ_{yyyy}	-7.15	-6.20	-5.90	-6.92	2.113712
γ_{yyzz}	3.86	3.15	3.00	3.39	1.279076
γ_{zzzz}	8.98	7.830	7.40	8.28	2.616517
γ_{zzzz}	1.27	1.27	1.27	1.27	1.27666
	1.06 x10^{-39}	**1.77 x10^{-39}**	**1.68 x10^{-39}**	**1.88 x10^{-39}**	**5.89 x10^{-40}**

The NLO properties of 3BAC were calculated using the density functional theoretical approach. Since α and γ values of the Gaussian output are reported in a. u., the calculated α and γ values were converted into the electrostatic units (esu) (1 a. u. α = 0.1482 × 10−24 esu, β: 1 a .u. = 8.6393 × 10−33 esu 1 a. u. γ = 5.0367 × 10−40 esu). The B3LYP6-311++G(d,p) results of the electric dipole moment μ, polarizability α_{ij} and the first hyperpolarizability β_{ijk}, second hyperpolarizability γ_{ijk} of the 3BAC are listed in Table 1d. The calculated dipole moment is equal to 2.81 D for 3BAC compound which is 1.52 D for reference NLO material KDP. It shows that the dipole moment is 1.84 times greater than the reference material KDP. The calculated dynamic polarizability α_{tot}, is equal to 2.57 x 10^{-23} esu for 3BAC which is 2.522.57 x 10^{-23} esu for reference KDP material. It shows that the dynamic polarizability is 1.01 times greater than the reference material KDP. The calculated first hyperpolarizability β_{tot} is equal to 1.01 x10^{-29} for 3BAC compound which is 8 x$10^{-31}$for reference NLO material KDP. It shows that the dipole moment is 1.26 times greater than the reference material KDP. The calculated second hyperpolarizability γ_{tot} is equal to 1.88 x10^{-39} for 3BAC compound which is 5.89 x10^{-40} for reference NLO material KDP. It shows that the dipole moment is 3.19 times greater than the reference material KDP. The obtained results show that the 3BAC molecule is an excellent material for NLO applications.

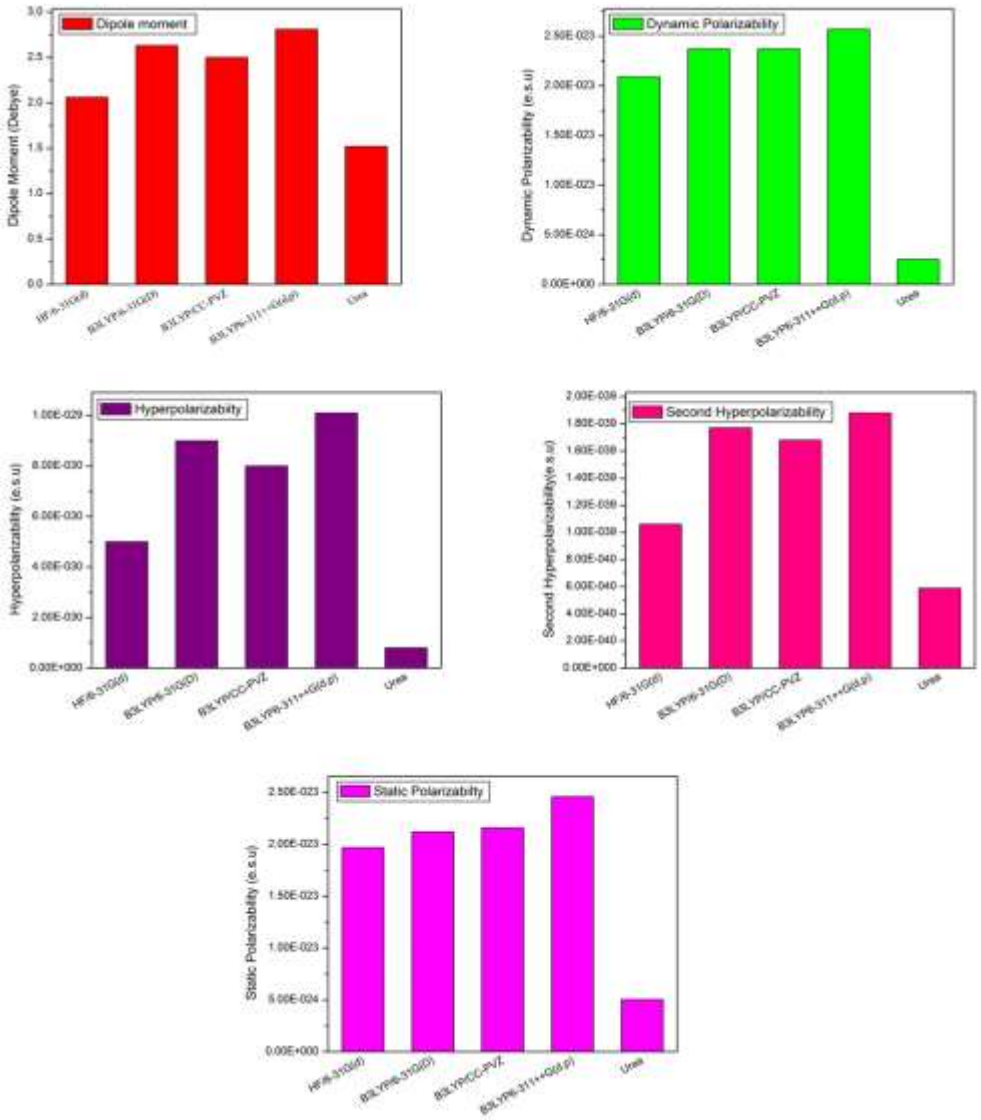

Figure 2: The variation on dipole moment, polariability and hyperpolarizabilities

IV. MOLECULAR ORBITAL STUDIES

The most widely used theory by chemists is the molecular orbital (MO) theory. It is important that Ionization Potential (I), Electronaffinity (A), Electrophilicity index (ω), Chemical Potential (μ), Electronegativity (χ), Hardness (η), and softness (S) be put into a MO framework. Based on density functional descriptors global chemical reactivity descriptors of compounds such as hardness, chemical potential, softness, electro negativity and electro philicity index as well as local Reactivity has been defined [37–38]. The above reactivity descriptors have been calculated using following equations (6)-(12) and listed in Table 2.

$$IP = E_{HOMO} \quad (6)$$

$$EA = E_{LUMO} \quad (7)$$

$$\chi = \frac{-(E_{HOMO}+E_{LUMO})}{2} \quad (8)$$

$$\mu = \frac{(E_{HOMO}+E_{LUMO})}{2} \quad (9)$$

$$\eta = (E_{LUMO}-E_{HOMO})2 \quad (10)$$

$$S = \frac{1}{2\eta} \quad (11)$$

$$\omega = \frac{\mu^2}{2\eta} \quad (12)$$

Table 2: Calculated Global reactivity descriptors using DFT/B3LYP/6-311++G(d,p)

HOMO	-7.323	
LUMO	-3.182	
Ioniztion Potnetial(IP)	IP= $-E_{HOMO}$	7.323
Electron Affinity (EA)	EA=$-E_{LUMO}$	3.182
Electronegativity (χ)	$\chi = \frac{-(E_{HOMO}+E_{LUMO})}{2}$	-5.2525
Chemical potential (μ)	$\mu = \frac{(E_{HOMO}+E_{LUMO})}{2}$	5.2525
Global Hardness(η)	$\eta = (E_{LUMO}-E_{HOMO})2$	2.0705
Softness (S)	$S = \frac{1}{2\eta}$	0.241488
Electrophilicity index (ω)	$\omega = \frac{\mu^2}{2\eta}$	6.662342

In the present case the calculated values of HOMO and LUMO are found to be -7.33 eV and -3.182 eV respectively. The energy gap between HOMO and LUMO is 4.141 eV. The ionization energy and electron affinity can are found to be 7.323 eV and 3.182 eV. The different global descriptors such as hardness, chemical potential and electrophilicity are also calculated for the most stable conformer and found to be 2.070, 5.252 and 6.66eV. Considering the chemical hardness, large chemical hardness expresses a hard molecule and small chemical hardness gap means a soft molecule. One can also relate the stability of molecule to hardness, which means that the molecule with least chemical hardness means it is more reactive.

V. MOLECULAR HIRSHFELD SURFACES:

A Hirshfeld surface analysis [39] was performed to visualize the different types of interactions present within a crystal structure using the Crystal Explorer 3.1 software [40] and the TONTO [38] system.

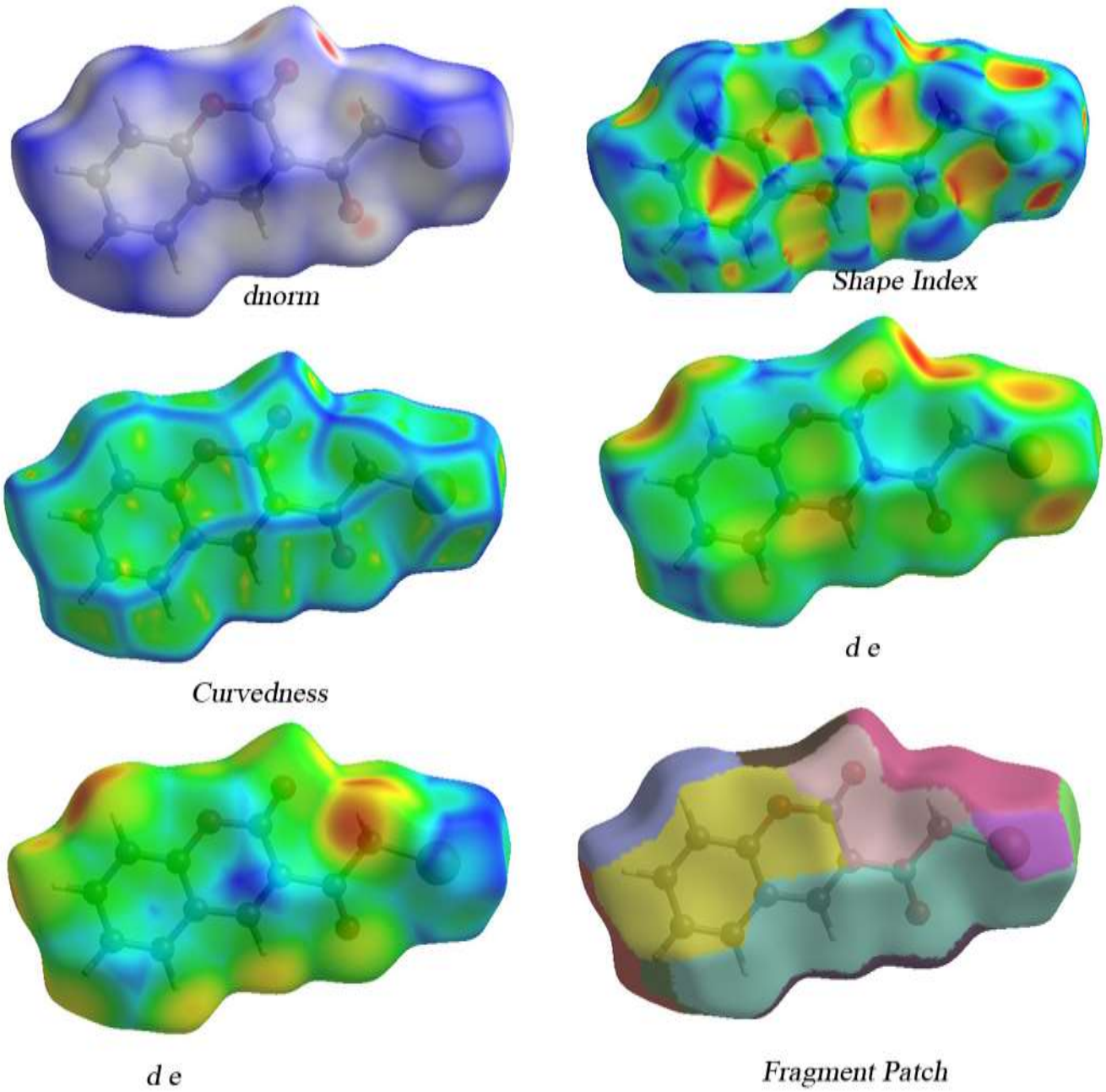

Figure 3: Molecular Hirshfeld surface; *dnorm*, d*e*, d*i*, *shape index* and *curvedne*ss for 3BAC

Hirshfeld surfaces are produced through the partitioning of space within a crystal where the ratio of promolecule to procrystal electron densities is equal to 0.5 and are mapped using the normalized contact distance (d_{norm}) which is defined in terms of external and internal distances $_{de}$ and $_{di}$ and the van der Waals (vdW) radii of atoms.

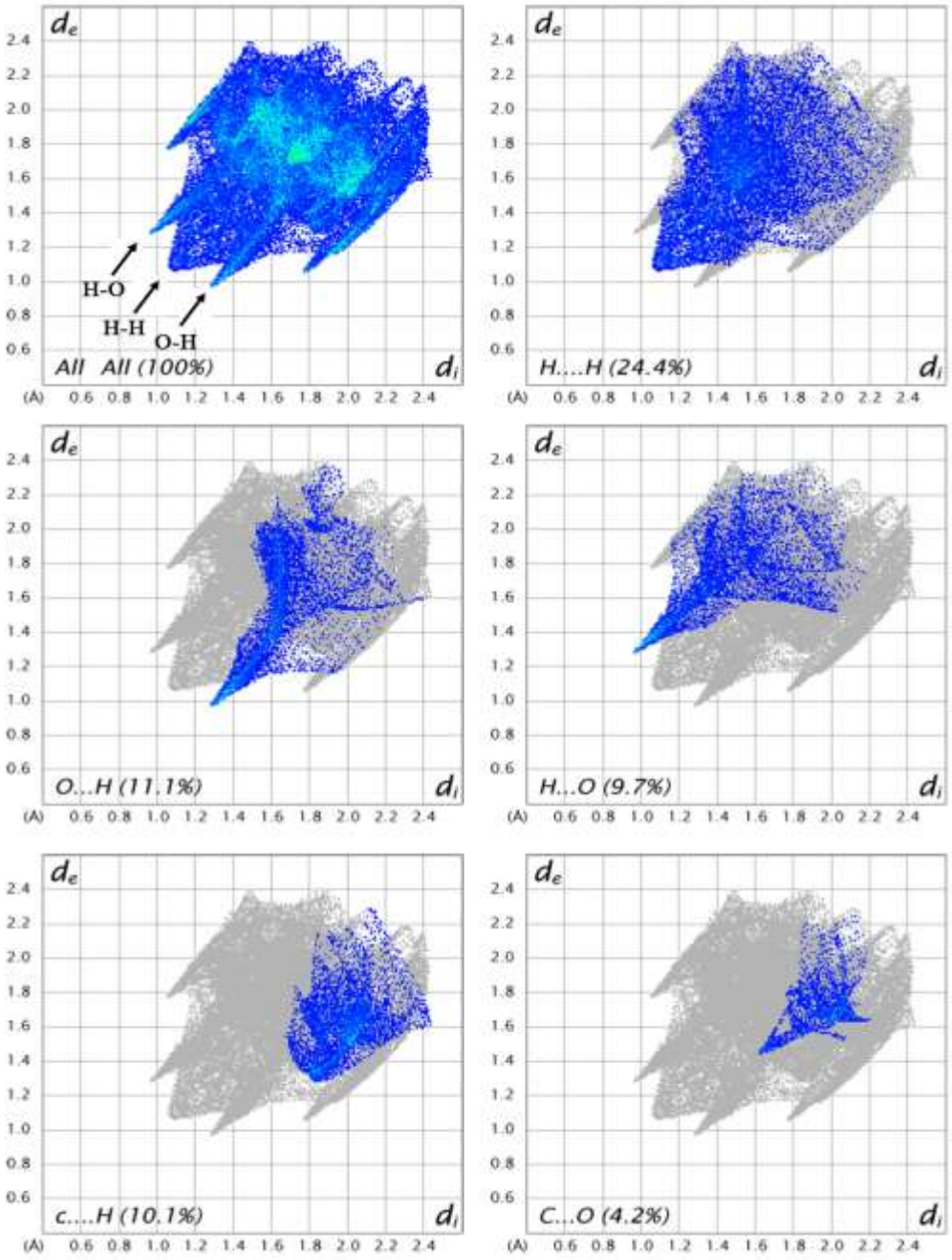

Figure 4: 2D fingerprint plots for 3BAC

The Hirshfeld surfaces are unique for a particular crystal structure and its numbers also depend on the number of crystallographically independent molecules in the corresponding asymmetric unit[41]. The molecular Hirshfeld surface; *dnorm*,*de*, d*i*,*shape index* and *curvedness* for3BAC is illustrated in Figures 3, respectively. From the result the surface mapped for a dnorm is ranges from -0.2521 to 0.9726Å, di, de are ranges form 0.9763 to -2.4549 Å and 0.9770 to-2.4505. The shape index ranges –1.0 to 1.0 Å, and curvedness ranges –4.0 to 4.0 Å, respectively. The dnorm mapping indicates that strong hydrogen bond interactions, such as C–H···O hydrogen bonding between C19-H10 and O18 atom.

The shape index is the most sensitive to very subtle changes in surface shape. From the the red triangles on them (above the plane of the molecule) represent by concave regions. indicating atoms of the π-stacked molecule above them, and the blue triangles represent by convex regions indicating the ring atoms of the molecule inside the surfaces. The red triangles on the shape index mapping are referring to the C-C···π interaction with the contribution of 5.0% and C-H…π contribution of 10.1% . The curvedness is a measure of the shape of the surface area of the molecule. The flat areas of the surface correspond to low values of curvedness, while sharp curvature areas correspond to high values of curvedness and usually tend to divide the surface into patches, indicating interactions between neighboring molecules. The large flat region which delineated by a blue outline refer to the π···π stacking interactions of C-C and C-H. The blue outline over the ring group indicate that the π···π stacking interaction is present over the ring group[42,43].

Table 3: Summary of various contacts and their contributions to the Hirshfeld Surface in 3BAC

Types of contacts	**Contributions in%**
C…C	5.0
C…H	10.1
H…C	6.2
H…H	24.4
O…H	11.1
H…O	9.7
H…Br	4.5
Br…H	10.1
O…Br	2.9
Br…O	4.2
C…Br	0.9
Br…C	1.1

The 2D fingerprint plots for 3BAC (Figure 4) show that the intermolecular H···H, C–H···O, O-H…..O and C–H···π interactions are well dominated and are in complement to the Hirshfeld surfaces. The fingerprint plots can also be decomposed to highlight particular atoms pair close contacts and enables separation of contributions from different interaction types. Two sharp spikes pointing towards lower left and right of the plot are typical O–H···O hydrogen bonds. This portion corresponds to H–O/O–H interactions comprising 20.8% of the total Hirshfed surfaces for each molecule of 3BAC. At the top left of the plot, there are characteristic “wings” which are identified as a result of C–H···π interactions. The decomposition of the fingerprint plots show that C–C contacts contribute 5.0% of the total Hirshfeld surface area for the molecule of 3BAC. They correspond to all C–H···C interactions of which C–H···π appear in the fingerprint plot in a characteristic manner. The broad region bearing short and narrow spikes at the middle of plot is reflected as H···H interaction in 3BAC comprising 24.4% of the total Hirshfeld surfaces for 3BAC. The other two sharp spikes pointing towards upper left and right of the plot are typical O–H···O hydrogen bonds. The presence of all interactions are summarized in Table 3.

VI. MOLECULAR DOCKING STUDY

Molecular docking is playing an increasingly important role in drug design for the treatment of many diseases. This technique provides insight into plausible protein-ligand interactions which can substantiate the experimental result.

Table 4: Docking parameters of the title compound docked into the active sites of the target proteins

Molecular docking-anti fungal				
Protein (PDB:ID)	**Binding Residue**	**Bond distance (Å)**	**Incubation constant (µm)**	**Binding affinity (k/cal)**
1cns	VAL 2	2.68	62.67	-5.7
	SER 3	1.83		
1bwa	ASN 59	1.91	**28.26**	**-6.2**
	ILE 58	1.91		
3f3h	SER 64	2.20	56.28	-5.8
Molecular docking-anti bacterial				
1loy	TYR 45	2.05	12.08	-6.7
	ASN 44	2.78		
	ASN 43	2.57		
2q0o	TYR 55	2.59	**2.23**	**-7.7**
1ktk	LYS 3	1.95	56.66	-5.8

For the identification of antibacterial and anti fungal activity the tittle compound is docked with different protein. For that anti fungal receptor (1cns, 1bwa and 3f3h) and antibacterial(1loy, 2q0o and 1ktk) receptors were selected from the Protein Data Bank(PDB). The Graphical User Interface program ‘‘Auto- Dock Tools’’ was used to prepare, run, and analyze the docking simulations. Kollman united atom charges, salvation parameters and polar hydrogen's were added to the receptor for the preparation of protein in docking simulation. Molecular docking software AutoDock 4.2.6 [44] Program supplied with AutoGrid 4.0 and AutoDock 4.0 was used to produce grid maps. During the docking process, a maximum of 100 conformers was considered for title compound.

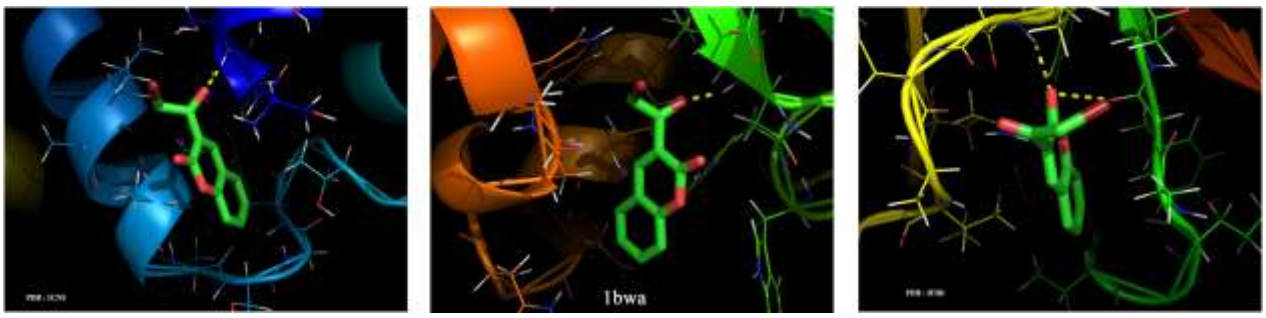

Figure 5: Binding Mode of the 1cns, 1bwa and 3f3h

For the ainti fungal studies the ligand was docked into the functional sites of the 1cns, 1bwa and 3f3h proteins individually and the docking energy was examined to achieve a minimum value. AutoDock results indicate the binding position and bound

conformation of the peptide, together with a rough estimate of its interaction. Docked conformation which had the lowest binding energy was chosen to investigate the mode of binding. The molecular docking binding energies (kcal/mol) and inhibition constants (mm) were also obtained and listed in Table 4. Among them, 1bwa exhibited the lowest binding energy at -6.2 kcal/mol and most docked inhibitors interacted with the ligand within the 1bwa binding site. The binding mode of the 1cns, 1bwa and 3f3h using the docking simulation are shown in Figure 5 The figure shows that the 1cns, 1bwa proteins binding through NH/O, hydrogen bond, and 3f3h protein binding through CO/H, hydrogen bond

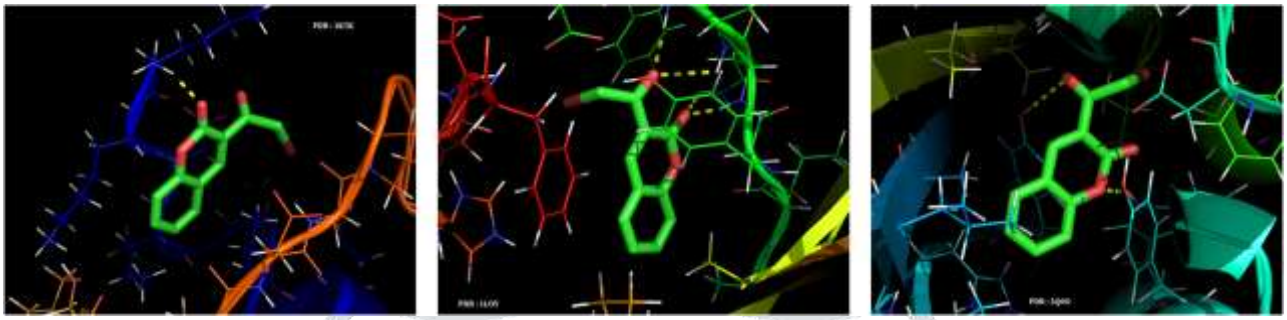

Figure 6: Binding Mode of the 1loy, 2q0o and 1ktk

In the same way for the ainti bacterial studies the ligand was docked into the functional sites of the 1loy, 2q0o and 1ktk proteins individually and the docking energy was examined to achieve a minimum value. AutoDock results indicate the binding position and bound conformation of the peptide, together with a rough estimate of its interaction. Docked conformation which had the lowest binding energy was chosen to investigate the mode of binding. The molecular docking binding energies (kcal/mol) and inhibition constants (mm) were also obtained and listed in Table 4. Among them, 1bwa exhibited the lowest binding energy at -7.7 kcal/mol and most docked inhibitors interacted with the ligand within the 2q0o a binding site. The binding mode of the 1loy, 2q0o and 1ktk using the docking simulation are shown in Figure 6. The figure shows that the 1ktk, proteins binding through one NH/O, hydrogen bond, 1loy proteins binding through three NH/O, hydrogen bond and 2q0o protein binding through NH/O and CO/H hydrogen bonds.

VII. ANTIBACTERIAL AND ANTIFUNGAL ACTIVITY

The antibacterial and antifungal potential of different dosages (10, 20 and 30 mg/mL) of HL was tested by disk diffusion method [45]. Disk diffusion tests were performed thrice and interpreted according to the recommendations of the Clinical and Laboratory Standards Institute [46]. Agar well diffusion method is widely used to evaluate the antimicrobial activity of the compound. Autoclaved 15-20 mL of Mueller-Hinton agar was poured on glass petri plates and allowed to solidify. Standardized inoculum of the test organism was uniformly spread on the surface of these plates using sterile cotton swab. Four wells with a diameter of 8 mm (20 mm apart from one another) were punched aseptically with a sterile cork borer in each plate. Sample (40 and 80µL) at desired concentration from 100mg/mL stock was added to twoof the wells and one well with Gentamycin as positive and compound solvent as negative control. Then, the agar plates were incubated under 37°C for 24 hrs. After incubation, clear zone was observed. Inhibition of the bacterial growth was measured in mm.

Table 5: Antibacterial and antifungal activity

Sample	***E.coli***				***A.niger***			
	+	**-**	**T1**	**T2**	**+**	**-**	**T1**	**T2**

3BAC	32	-	26	30	20	-	30	35

The results of two habitually infection causing bacterial strains E. coli indicate that bacterial species exhibit different sensitivities towards the HL, required results has been compared with the inhibition diameter of positive control. In the E. coli strain the inhibitor zone was formed with a certain mm distance. It shows that the tested title compound possess appreciable antibacterial activity and is shown in Figure 7. The results of two habitually infection causing fungal strains A.niger indicate that fungal species exhibit different sensitivities towards the HL, required results has been compared with the inhibition diameter of positive control.

Figure 7: Appreciable antifungal activity

In the A.niger strain the inhibitor zone was formed with a certain mm distance. It shows that the tested title compound possess appreciable antifungal activity and is shown in Figure 7 respectively. The tested antibacterial and antifungal activity of the title compound is given in the Table5

VIII. CONCLUSIONS

The optimized structure of 3 BAC was calculated at DFT/B3LYP level with 6-311++G(d,p) basis set. The optimized structure shows the minimum energy confirmation. The theoretical nonlinear optical parameters such as dipole moment, polarizability, Hyperpolarizability and hyperpolarizability of the title compound was calculated and analyzed. The result evidence the possibility intra molecular charge transfer interaction and of presence of NLO activity of the molecule. The molecular Hirshfeld analysis was also done to identify the contribution of interaction which responsible of biological or NLO activity. The global reactivity such chemical potential of compound is (μ= -5.2525 eV), chemical hardness (η=2.0705 eV), softness (S=2.164 eV), ionization energy (S=00.241488 eV), electron affinity (EA=3.182 eV), electronegativity (χ = -5.2525 eV) were calculated and analyzed. The biological activity of the compound was identified using the Docking software and it was confirmed by the experimental anti fungal and anti bacterial activities.

References:

1. http://dx.doi.org/10.1016/j.ica.2012.11.010 http://micro.magnet.fsu.edu/phytochemicals/pages/coumarin.html.
2. http://en.wikipedia.org/wiki/Coumarin.
3. J.T. Brett, J. Alexander, M.J.J. Stezowski, Chemical insight from crystallographic disorder-structural studies of supramolecular photochemical systems. Part 2. The beta-cyclodextrin-4,7-dimethylcoumarin inclusion complex: a new beta-cyclodextrin dimer packing type, unanticipated photoproduct formation, and an examination of guest influence on beta-CD dimer packing J. Chem. Soc. Perkin Trans. 2 (2000) 1095–1103.

4. K. Vishnumurthy, T.N. Guru Row, K. Venkatesan, "Fluorine in crystal engineering:
5. photodimerization of(1E,3E)-4-pentafluorophenylbuta-1, 3-dienes in the crystalline state". Photochemistry (2001) 427–460.
6. N.A. Nemkovich, H. Reis, W. Baumann, "Ground and excited state dipole moments of coumarin laser dyes: Investigation by electro-optical absorption and emission methods"J. Lumin. 71 (1997) 255–263.
7. V.K. Sharma, P.D. Saharo, N. Sharma, R.C. Rastogi, "Influence of solvent and substituent on excited state characteristics of laser grade coumarin dyes"Spectrochim. Acta A 59 (2003) 1161–1170.
8. S. Sardari, Y. Mori, K. Horita, R.G. Micetich, S. Nishibe, M. Daneshtalab, "Synthesis and antifungal activity of coumarins and angular furanocoumarins"Bioorg. Med. Chem. 7 (1999) 1933–1940.
9. M.B. Maria, Z.Y. Wang, "Short communicationFull text access
10. A dual-mode molecular switch based on a chiral binaphthol-coumarin compound"Tetrahedron Lett. 41 (2000) 4025–4028.
11. J.M. Domagala, S.E. Hagen, E.T. Lunney, D. Bradly, Warner-Lambert Co. USA, US Patent No. 5 (1996) 5103 75.
12. A.I. Eid, F.A. Ragab, S.L. El-Ansary, S.M. El-Gazayerly, F.E. Mourad, "Synthesis of New 7-Substituted 4-Methylcoumarin Derivatives of Antimicrobial Activity"Arch. Pharm. 327 (1994) 211–213.
13. J.W. Suttie, "Warfarin and vitamin K."Clin. Cardiol. 13 (1990) 16-18
14. C.T. Supuran, "Complexes With Biologically Active Ligands. Part 1. Synthesis of Coordination Compounds of Diazoxide With Transition- and Main-Group Cations"ligands 3 (1996) 25–30.
15. P.N. Prasad, D.J. Williams, Introduction to Nonlinear Optical Effects in Organic Molecules and Polymers, Wiley, New York, 1991.
16. Z. Kotler, R. Hierle, D. Josse, J. Zyss, R. Masse, Quadratic nonlinear-optical properties of a new transparent and highly efficient organiceinorganic crystal: 2-amino-5-nitropyridinium-dihydrogen phosphate (2A5NPDP), J. Opt. Soc. Am. B 9 (1992) 534-547.
17. N. Horiuchi, F. Lefaucheux, A. Ibanez, D. Josse, J. Zyss, Quadratic nonlinear optical coefficients of organic-inorganic crystal: 2-amino-5-nitropyridinium chloride, J. Opt. Soc. Am. B 19 (2002) 1830-1838.
18. S. Manivannan, S. Dhanuskodi, K. Kirschbaum, S.K. Tiwari, Design of an efficient solution grown semiorganic NLO crystal for short wavelength generation: 2-amino-5-nitropyridinium tetrafluoroborate, Cryst. Growth Des. 5 (2005) 1463-1468.
19. W. Bi, N. Louvain, N. Mercier, J. Luc, I. Rau, F. Kajzar, B. Sahraoui, A switchable NLO organic-inorganic compound based on conformationally chiral disulfide molecules and Bi (III) I5 iodobismuthate networks, Adv. Mater 20 (2008) 1013e1017.
20. P. Calaminici, K. Jug, A.M. Köster," Density functional calculations of molecular polarizabilities and hyperpolarizabilities" J. Chem. Phys. 109 (1998) 7756.
21. P. Salek, T. Helgaker, O. Vahtras, H. Agren, D. Jonsson, J. Gauss, "A comparison of density-functional-theory and coupled-cluster frequency-dependent polarizabilities and hyperpolarizabilities"Mol. Phys. 103 (2005) 439-450.
22. D.P. Shelton, J.E. Rice, "Measurements and calculations of the hyperpolarizabilities of atoms and small molecules in the gas phase"Chem. Rev. 94 (1994) 3.
23. C.M. Isborn, A. Leclerq, F.D. Vila, L.R. Dalton, J.L. Bredas, B.E. Eichinger, B.H. Robinson, J. Phys. Chem. A 111 (2007) 1319.
24. M.J. Frisch et al., Gaussian 09W Program, Gaussian Inc., Wallingford, CT, 2009.
25. P. Hohenberg, W. Kohn," Inhomogeneous Electron Gas" Phys. Rev. 136B (1964) 864–871.
26. A.D. Becke, "Density-functional thermochemistry. III. The role of exact exchange"J. Chem. Phys. 98 (1993) 5648–5652.
27. C. Lee, W. Yang, R.G. Parr," Development of the Colle-Salvetti correlation-energy formula into a functional of the electron density" Phys. Rev. B 37 (1998) 785–789.
28. C.R. Zhang, H.S. Chem, G.H. Wang, "Geometry, Electronic Structure, and Related Properties of Dye Sensitizer: 3,4-bis[1-(carboxymethyl)-3-indolyl]-1H-pyrrole-2,5-dione"Chem. Res. Chin. Uni. 20 (2004) 640.
29. G.M. Morris, D.S. Goodsell, R.S. Halliday, R. Huey, W.E. Hart, R.K. Belew, A.J. Olson, Automated docking using a lamarckian genetic algorithm and empirical binding free energy function, J. Comput. Chem. 19 (1998) 1639-1662.D. Buckingham, Adv. Chem. Phys. 12 (1967) 107.

30. O. Christiansen, J. Gauss, J.F. Stanton, "Frequency-dependent polarizabilities and first hyperpolarizabilities of CO and H2O from coupled cluster calculations"Chem. Phys. Lett. 305 (1999) 147-155.
31. N. Bloembergen, Nonlinear Optics, Benjamin, New York, **1965**.
32. N.F. Lane, "The theory of electron-molecule collisions"Rev. Mod. Phys. 52 (1980) 29.
33. G. Birnbaum (Ed.), Phenomena Induced by Intermolecular Interactions, Plenum, New York, **1980**.
34. J.B. Foresman, A. Frisch, Exploring Chemistry with Electronic Structure Methods, Gaussian Inc., Pittsburgh, 1996.
35. M.J. Frisch, J.A. Pople, J.S. Binkley," Self-consistent molecular orbital methods Supplementary functions for Gaussian basis sets" J. Chem. Phys. 80 (1984) 3265–3269.
36. D.A. Kleinmen, "Nonlinear Dielectric Polarization in Optical Media"Phys. Rev. 126 (1962) 1977.
37. R.G. Parr, L.V. Szentpaly, S.J. Liu," Electrophilicity Index" Am. Chem. Soc. 121 (1999) 1922–1924.
38. P.K. Chaltraj, B. Maiti, U.J. Sarbar, J. Phys. Chem. A 107 (2003) 4973–4975.
39. J.J. McKinnon, D. Jayatilaka, M.A. Spackman, Chem. Commun. (2007) 3814-3816.
40. S.K. Wolff, D.J. Grimwood, J.J. McKinnon, M.J. Turner, D. Jayatilaka, M.A. Spackman, Crystal-explorer 3.1, University of Western Australia, Perth,2012
41. J. J. McKinnon, F. P. A. Fabbiani, M. A. Spackman, Cryst. Growth Des. 2007, 7, 755–769. http://dx.doi.org/10.1021/cg060773k
42. Y.-H. Luo, G.-G. Wu, S.-L. Mao, B.-W. Sun, "Complexation of different metals with a novel N-donor bridging receptor and Hirshfeld surfaces analysis "Inorg. Chim. Acta 2013, 397, 1-9.http://dx.doi.org/10.1016/j.ica.2012.11.010
43. Y. Li, C. -G. Zhang, L. -Y. Cai, Z. -X. Wang, "Synthesis, crystal structure, Hirshfeld surfaces, and spectral properties of Cu(II) and Co(II) complexes with 3-phenoxymethyl-4-phenyl-5-(2-pyridyl)-1,2,4-triazole"J. Coord. Chem. 2013, 66, 3100–3112. http://dx.doi.org/10.1080/00958972.2013.826350
44. O. Trott, A.J. Olson, "AutoDock Vina: improving the speed and accuracy of docking with a new scoring function, efficient optimization, and multithreading"J. Comput. Chem. 31 (2010) 455.
45. A.W. Bauer, W.M. Kirby, J.C. Sherries, M. Turckp, "Antibiotic susceptibility testing by a standardized single disk method"Am. J. Clin. Pathol. 45 (1966)493-496.
46. P.A. Wayne, Clin. Lab. Std. Inst. 34 (2014) 50-57.